International Journal of Heavy Vehicle Systems

ISSN online: 1741-5152 - ISSN print: 1744-232X
https://www.inderscience.com/ijhvs

Hardware-in-the-loop simulation of active roll control for single-trailer truck using steerable wheel at the middle axle

Muhammad Nadwi Hakimi Adnan, Zulkiffli Abd Kadir, Khisbullah Hudha, Noor Hafizah Amer, Mohd Sabirin Rahmat, Mohamad Hafiz Harun, Vimal Rau Aparow

DOI: 10.1504/IJHVS.2023.10057364

Article History:

Received:	05 June 2021
Last revised:	03 September 2021
Accepted:	07 September 2021
Published online:	06 July 2023

Hardware-in-the-loop simulation of active roll control for single-trailer truck using steerable wheel at the middle axle

Muhammad Nadwi Hakimi Adnan,
Zulkiffli Abd Kadir*, Khisbullah Hudha
and Noor Hafizah Amer

Faculty of Engineering,
Universiti Pertahanan Nasional Malaysia,
57000, Kuala Lumpur, Malaysia
Email: nadwiad6@gmail.com
Email: zulkiffli@upnm.edu.my
Email: k.hudha@upnm.edu.my
Email: noorhafizah@upnm.edu.my
*Corresponding author

Mohd Sabirin Rahmat

Faculty of Engineering and Built Environment,
Department of Mechanical Engineering,
MAHSA Univeristy, Jalan SP 2, Bandar Saujana Putra,
42610, Jenjarom, Selangor
Email: sabirin.rahmat@gmail.com

Mohamad Hafiz Harun

Faculty of Mechanical and Manufacturing Engineering Technology,
Universiti Teknikal Malaysia Melaka,
76100, Durian Tunggal, Melaka, Malaysia
Email: mohamadhafiz@utem.edu.my

Vimal Rau Aparow

Faculty Electrical and Electronic Engineering,
University of Nottingham,
Malaysia Campus, 43500, Semenyih, Selangor, Malaysia
Email: vimal.rau@nottingham.edu.my

Abstract: Normally, a single-trailer truck will lose its manoeuvrability when driving at a high speed during cornering or sudden lane changing manoeuvres. In order to improve the manoeuvrability and to avoid rollover accident, this study proposes an active roll control (ARC) using steerable-wheel system at middle axle for single-trailer truck. The system is developed to reject the unwanted yaw, lateral and roll motions based on trailer responses. The control structure of the ARC system is developed on a verified 18-DOF of single-trailer truck model. PID controller as trailer's roll angle feedback control is applied in the control structure and additional roll moment cancellation control using skyhook controller. From the experimental results using hardware-in-the-loop simulation (HiLS), a good similarity between simulation and experiment is observed for yaw rate, roll angle and lateral acceleration responses. It also shows that the developed steerable-wheel system was managed to reduce the unwanted lateral, yaw and roll motions.

Keywords: middle axle steerable wheel; truck-trailer; ARC; active roll control; HiLS; hardware-in-the-loop simulation; PID-skyhook.

Reference to this paper should be made as follows: Adnan, M.N.H., Kadir, Z.A., Hudha, K., Amer, N.H., Rahmat, M.S., Harun, M.H. and Aparow, V.R. (2023) 'Hardware-in-the-loop simulation of active roll control for single-trailer truck using steerable wheel at the middle axle', *Int. J. Heavy Vehicle Systems*, Vol. 30, No. 1, pp.90–118.

Biographical notes: Muhammad Nadwi Hakimi Adnan received his BE in Mechanical Engineering Department, Universiti Pertahanan Nasional Malaysia (UPNM). His research interests include vehicle dynamics, modelling and control. His recent research interests in modelling and active roll control for truck vehicles.

Zulkiffli Abd Kadir received his BE and MSc in the Department of Automotive Engineering, Universiti Teknikal Malaysia Melaka. Then, obtained his PhD from Universiti Teknologi Malaysia (UTM) on Development of Active Front Wheel Vehicle System. His research interests include tyre modelling, evaluation of vehicle dynamics and control. He is currently attached with the Universiti Pertahanan Nasional Malaysia and actively involved in vehicle modelling, system identifications and intelligent control system for the vehicle active safety system.

Khisbullah Hudha received his BE in Mechanical Design from Bandung Institute of Technology (ITB), Indonesia; MSc in the Department of Engineering Production Design from Technische Hoogeschool Utrecht at Netherlands and his PhD in Intelligent Vehicle Dynamics Control using Magnetorheological Damper from Universiti Teknologi Malaysia (UTM). His research interests include modelling, identification and force tracking control of semi-active damper, evaluation of vehicle ride and handling, electronic chassis control system design and intelligent control. He is currently attached as Associate Professor with Universiti Pertahanan Nasional Malaysia (UPNM) and actively involved in parallel hybrid vehicle and active safety system for military armoured vehicle.

Noor Hafizah Amer received her first degree, ME (Hons) in Mechanical Engineering (Automotive) from The University of Nottingham, UK and MEngSc in Mechanical Engineering, Universiti Malaya, Malaysia. She is currently attached as an academic staff with the Universiti Pertahanan Nasional Malaysia (UPNM) and a PhD holder from Universiti Teknologi Malaysia (UTM). Her research interests include vehicle control system, automotive suspension, optimisation and autonomous vehicle.

Mohd Sabirin Rahmat received his BE and MSc from Faculty of Mechanical Engineering, University Teknikal Malaysia Melaka (UTeM). Then, obtained his PhD from Universiti Pertahanan Nasional Malaysia (UPNM). He is currently attached as an Academic Staff with the MAHSA Univeristy, Malaysia and his research primarily focuses on semi-active damper systems for impact loadings application, hybrid electric vehicle and vehicle dynamic, modelling and control. His recent research interests include in modelling and characterisation of semi-active damper system for gun recoil stabilisation system.

Mohamad Hafiz Harun received his BE from the Department of Automotive Engineering, Faculty of Mechanical Engineering, Universiti Teknologi Malaysia (UTM), MSc from Universiti Teknikal Malaysia Melaka (UTeM) and PhD from Universiti Teknologi Malaysia. He is currently a Senior Lecturer in the Faculty of Mechanical and Manufacturing Engineering Technology at Universiti Teknikal Malaysia Melaka. His research currently focuses on the development of a rollover warning system for commercial vehicle.

Vimal Rau Aparow received his BE and MSc in the Department of Automotive, Faculty of Mechanical Engineering, Technical University of Malaysia Malacca (UTeM). Then, obtained his PhD from Universiti Pertahanan Nasional Malaysia (UPNM). His research primarily focuses on active safety system for military armoured vehicle, active braking system and hybrid vehicles. His recent research interests include in vehicle modelling, brake modelling, system identifications and intelligent control system for the vehicle active safety system.

1 Introduction

Generally, lateral acceleration causes lateral load transfer within the single-trailer trucks body from its centre of gravity (CG) and shifted outwards during cornering manoeuvres (Ali et al., 2017; Sert and Boyraz, 2017). This produces an unwanted roll motion and directly reduces the roll stability during cornering manoeuvres (Ramakrisna et al., 2017; He et al., 2019). Rollover incidents on trucks can be divided into two categories namely tripped rollover which is due to huge external vertical forces that induced to the vehicle and untripped rollover that due to responses from the truck in extreme road turning at a high speed manoeuvring (Han and Rho, 2017; Kazemian et al., 2017; Ataei et al., 2019). In order to overcome the untripped rollover issues on trailer-trucks, many automotive researches have been initiated in focusing on modelling of the single-trailer trucks system using mathematical and multi-body approaches to investigate the behaviours of the vehicle in various manoeuvrings. Most of the researchers have expanded their research interests towards the development of active rollover prevention system or commonly known as anti-rollover system using real-time estimation of roll angle, active suspension system, active stabiliser bar, electronic stability system and prediction algorithms for anti-rollover system (Rahimi and Naraghi, 2018; Chen et al., 2019).

In this study, a new concept of active safety system known as active roll control (ARC) using steerable-wheel (SW) at middle axle of single-trailer truck is proposed and implemented into a verified full single-trailer truck model. The single-trailer truck model consists of 18-degree-of-freedom (18-DOF) connected with a hitch joint model using a set of differential equations and merged with a Calspan tyre model as explained by Ahmad et al. (2010). The selection of Calspan tyre model is due to its ability in representing the characteristic of the vehicle in any driving conditions (Adnan et al., 2020). In order to verify the validity of the developed model, a model verification procedure through simulation process was carried out using a well-known heavy vehicle dynamics software namely TruckSim. The model verification process was defined as the level of agreement of both responses between the developed model and TruckSim based on the similar manoeuvring test. Two types of handling test namely single lane change (SLC) and double lane change (DLC) tests at 60 km/h and 80 km/h were conducted using the similar truck's parameters in TruckSim software. Several single-trailer truck's responses were observed to verify the level of model's agreement against the TruckSim software namely roll angle, yaw rate and lateral acceleration. The modelling process and detailed derivation of the developed model and its verification results have been done in the author's previous manuscripts (Adnan et al., 2020; Yussof et al., 2020).

The development of ARC in this study is based on trailer's responses that can be used to cancel out the unwanted lateral, yaw and roll motions for preventing the truck from rollover. The selection of trailer's responses as the controller feedbacks are due to most of the rollover accidents of the truck-trailer vehicle caused by the trailer due to its load and characteristics (Kemp et al., 1978). In addition, the trailer has a behaviour to self-excited in lateral direction due to disturbance namely rearward amplification (RWA) (Ni et al., 2020). Here, a new approach for active safety system is proposed with a new controller structure for ARC system using steerable wheel (SW) for the middle axle. The SW is operated by the ARC controller, and its capability in improving the roll stability in the single-trailer truck vehicle are observed in both simulation and experiment using hardware-in-the-loop simulation (HiLS) approach. Apart from the designing the proposed ARC using SW, another contribution of the control structure is developed based on two outer loop feedbacks namely roll angle using PID controller and additional roll moment cancellation control using a set of linear and rotary imaginary dampers known as skyhook controller that implemented on the trailer. PID feedback controller is used to minimise the unwanted yaw, roll and lateral motions, while the additional roll moment cancellation controller is used to cancel out the unwanted load transfer of the trailer due to steering input from driver. The appropriate angle produced by the both controller feedbacks are then used as the target angle by inner loop controller for SW actuator. Here, the effectiveness of the proposed SW that actuated by the ARC using PID-Skyhook controller in cancelling out the unwanted roll motion during cornering manoeuvres is evaluated via HiLS using single-trailer truck test rig. The developed test rig also can be used to evaluate the benefits of the proposed system in any driving situations (Ružinskas and Sivilevičius, 2017; Žuraulis and Kilikevičius, 2019).

This manuscript is organised as follows: An introduction of single-trailer truck modelling and verification process as well as the main work of this manuscript is presented in Section 1. Section 2 describes the approach in modelling the single-truck trailer. Detailed information on development of ARC is described in Section 3 and followed by the simulation results in Section 4. Sections 5 and 6 present the results of experimental work on steerable-wheel actuator and ARC using HiLS test. Finally, the finding obtained in this study is shown in the conclusion section.

2 Development of 18 degree-of-freedoms of a single-trailer truck model with hitch joint

The six-wheeled single-trailer truck model considered in this study is categorised as a commodities carrier with 3-axle system as illustrated in Figure 1. The 18-DOF single-trailer truck model consists of 9-DOF truck and 9-DOF of trailer models. Both models are developed based on several subsystems which are handling, ride and Calspan tyre models with the dynamics function of tyre slip angle and longitudinal slip, respectively. The responses of trailer are based on the motion of the truck that connected using a hitch joint model. Combination of all subsystems allowing the single-trailer truck body to roll, pitch and heave about the longitudinal, lateral and vertical axes, respectively and also producing the lateral, longitudinal and yaw motions.

Figure 1 A 2D view of single-trailer truck (see online version for colours)

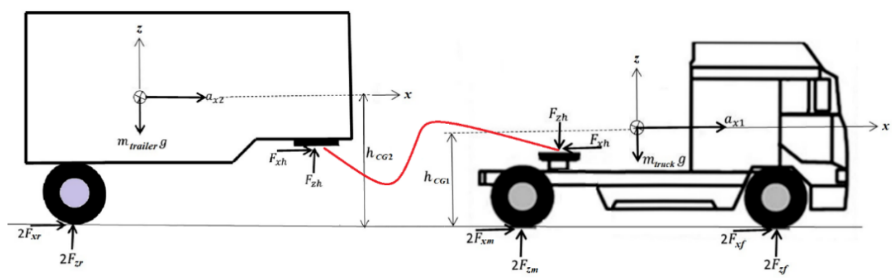

There are several modelling assumptions considered in constructing the 18-DOF single-trailer truck model namely:

- each suspension system is developed as linear spring and damper (Barethiye et al., 2017; Yoon et al., 2021)
- the hitch joint is modelled using a set of differential equations
- the effect of the truck-trailer's rolling resistance from passive anti-roll bar is taken into account in the mass moment of inertia about the longitudinal axis
- each tyre is modelled as a linear spring (Hamed and Elrawemi, 2018)
- each tyre maintains in contact with the ground at all times during manoeuvring
- the truck-trailer is travelling on a flat road with negligible road irregularities (Li et al., 2019)
- the truck-trailer is free to move along the lateral and longitudinal directions as well as to rotate about the vertical axis
- the effect of aerodynamic in longitudinal direction is not considered and the single-trailer truck is set to travel at a constant speed (Salaani and Elsasser, 2017).

2.1 Mathematical derivation of truck ride and handling models

The 12 degree-of-freedom (12-DOF) single-trailer truck ride model in Figure 2 consists of two sprung masses which are the truck and the trailer bodies. The truck body is connected to four unsprung masses located on the front right, front left, rear right, and rear left of each truck wheel. The trailer body has two unsprung masses on the right and left of each wheel. Each sprung mass is free to pitch and roll, and vertical motions of all unsprung masses are in the *z*-axis. All the tyres are assumed to have similar stiffness and modelled as linear spring without damping.

Figure 2 Single-trailer truck ride model (see online version for colours)

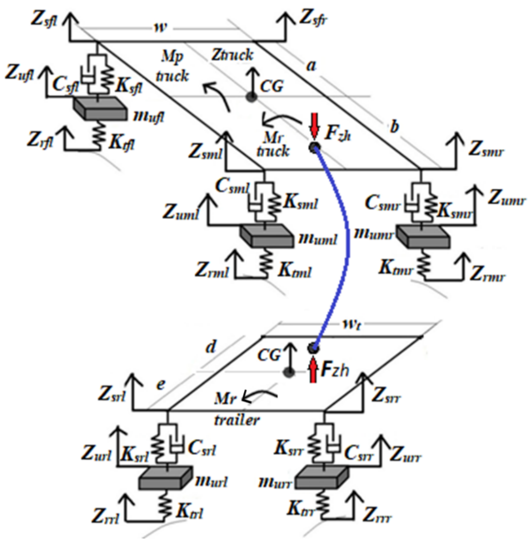

The truck's equation of motion when considering the forces acting on the sprung mass is as follows.

$$F_{sfl} + F_{dfl} + F_{sfr} + F_{dfr} + F_{sml} + F_{dml} + F_{smr} + F_{dmr} - F_{zh} = m_{t1}\ddot{Z}_{truck} \quad (1)$$

where

$\ddot{Z}_{truck}$ = vertical acceleration of truck at CG

m_{t1} = weight of truck sprung mass truck

F_{zh} = hitch vertical force

F_{sfr} = front right spring force = $K_{sfr}(Z_{ufr} - Z_{sfr})$

F_{sfl} = front left spring force = $K_{sfl}(Z_{ufl} - Z_{sfl})$

F_{smr} = middle right spring force = $K_{smr}(Z_{umr} - Z_{smr})$

F_{sml} = middle left spring force = $K_{sml}(Z_{uml} - Z_{sml})$

F_{dfr} = front right damper force = $C_{sfr}(\dot{Z}_{ufr} - \dot{Z}_{sfr})$

F_{dfl} = front left damper force = $C_{sfl}(\dot{Z}_{ufl} - \dot{Z}_{sfl})$

F_{dmr} = middle right damper force = $C_{smr}(\dot{Z}_{umr} - \dot{Z}_{smr})$

F_{dml} = middle left damper force = $C_{sml}(\dot{Z}_{uml} - \dot{Z}_{sml})$

$K_{sfr}, K_{sfl}, K_{smr}, K_{sml}$ = spring stiffness at the front right, front left, middle right and middle left.

$C_{sfr}, C_{sfl}, C_{smr}, C_{sml}$ = damping stiffness at the front right, front left, middle right and middle left.

$Z_{sfr}, Z_{sfl}, Z_{smr}, Z_{sml}$ = sprung masses displacement at the front right, front left, middle right and middle left.

$Z_{ufr}, Z_{ufl}, Z_{umr}, Z_{uml}$ = unsprung masses displacement at the front right, front left, middle right and middle left.

$\dot{Z}_{sfr}, \dot{Z}_{sfl}, \dot{Z}_{smr}, \dot{Z}_{sml}$ = sprung masses velocity at the front right, front left, middle right and middle left.

$\dot{Z}_{ufr}, \dot{Z}_{ufl}, \dot{Z}_{umr}, \dot{Z}_{uml}$ = unsprung masses velocity at the front right, front left, middle right and middle left.

Equation of roll dynamic motion is given as,

$$I_{roll1}\ddot{\phi}_1 = \left(F_{sfr} + F_{smr} + F_{dfr} + F_{dmr}\right)\frac{w}{2} - \left(F_{sfl} + F_{sml} + F_{dfl} + F_{dml}\right)\frac{w}{2} + m_{truck}a_{y1}h_{CG1} \quad (2)$$

where

$\ddot{\phi}_1$ = truck roll angular acceleration

I_{roll1} = moment inertia of roll axis

a_{y1} = truck lateral acceleration

h_{CG1} = distance from ground to CG

w = truck track width

Similarly, moment balance equation for truck pitch motion is given as,

$$\begin{aligned} I_{pitch1}\ddot{\theta}_1 = {} & \left(F_{smr} + F_{dmr} + F_{sml} + F_{dm1}\right)b - \left(F_{sfr} + F_{dfr} + F_{sfl} + F_{dfl}\right)a \\ & - \left(F_{zh}\right)c + m_{truck}a_{x1}h_{CG1} \end{aligned} \quad (3)$$

where,

$\ddot{\theta}_1$ = truck pitch angular acceleration

I_{pitch1} = moment inertia of pitch axis

a = distance from the body CG to front tyre

b = distance from the body CG to front tyre

c = distance from the body CG to hitch joint

a_{x1} = longitudinal acceleration of truck

Next, the trailer ride model that consists of two wheels on the rear axle is derived using the similar approach. The equation of motion for the trailer sprung mass is as follows.

$$F_{srl} + F_{drl} + F_{srr} + F_{drr} + F_{zh} = m_{t2}\ddot{Z}_{trailer} \tag{4}$$

The suspension forces for the trailer ride model are as follows.

$$F_{srl} = K_{srl}(Z_{url} - Z_{srl}) \tag{5}$$

$$F_{drl} = C_{srl}(\dot{Z}_{url} - \dot{Z}_{url}) \tag{6}$$

$$F_{srr} = K_{srr}(Z_{urr} - Z_{srr}) \tag{7}$$

$$F_{drr} = C_{srr}(\dot{Z}_{urr} - \dot{Z}_{urr}) \tag{8}$$

The equation for calculating the pitch and roll motions of the trailer is as follows.

$$I_{pitch2}\ddot{\theta}_2 = (F_{srr} + F_{drr} + F_{srl} + F_{drl})e - F_{zh}(d) + m_{trailer}a_{x2}h_{CG2} \tag{9}$$

$$I_{roll2}\ddot{\phi}_2 = \left(F_{srr} + F_{drr} - F_{srl} - F_{drl}\right)\frac{wt}{2} + m_{trailer}a_{y2}h_{CG2} \tag{10}$$

The next process is modelling the single-trailer truck handling model. Figure 3 illustrates the single-trailer truck handling which has a 6-DOF for vehicle's longitudinal, lateral and rotational yaw motions for both truck and trailer. Input of the model is obtained from the front wheel angle (δ) and the vehicle speed to produce the magnitude of longitudinal acceleration at x-axis, lateral acceleration at y-axis and the yaw angular acceleration at z-axis.

Based on the truck handling model in Figure 3, the equations for the longitudinal motion (a_{x1}) in the x-direction, the lateral acceleration (a_{y1}) in the y-direction, and the yaw motion in the vertical axis of the truck are as follows.

$$m_{truck}a_{x1} = \begin{bmatrix} F_{xmr} + F_{xml} + F_{yfr}sin\delta + F_{xfr}cos\delta + F_{yfl}sin\delta \\ +F_{xfl}cos\delta - F_{xh}cos\beta - F_{yh}sin\beta \end{bmatrix} \tag{11}$$

$$m_{truck}a_{y1} = \begin{bmatrix} F_{ymr} + F_{yml} + F_{xfr}sin\delta - F_{yfr}cos\delta + F_{xfl}sin\delta \\ -F_{yfl}cos\delta - F_{xh}sin\beta + F_{yh}cos\beta \end{bmatrix} \tag{12}$$

$$I_{ztruck}\ddot{r}_{truck} = \begin{bmatrix} \frac{w}{2}F_{xfr}cos\delta - \frac{w}{2}F_{xfl}cos\delta + \frac{w}{2}F_{xmr} - \frac{w}{2}F_{xml} - \frac{w}{2}F_{yfl}sin\delta \\ +\frac{w}{2}F_{yfr}sin\delta + bF_{yml} + bF_{ymr} - aF_{yfl}cos\delta - aF_{yfr}cos\delta \\ +aF_{xfl}sin\delta + aF_{xfr}sin\delta + cF_{yh}cos\beta - cF_{xh}sin\beta \end{bmatrix} \tag{13}$$

where

δ = Steering wheel angle

m_{truck} = Mass of the truck

I_{ztruck} = Yaw inertia of the truck.

Figure 3 7-DOF single-trailer truck model (see online version for colours)

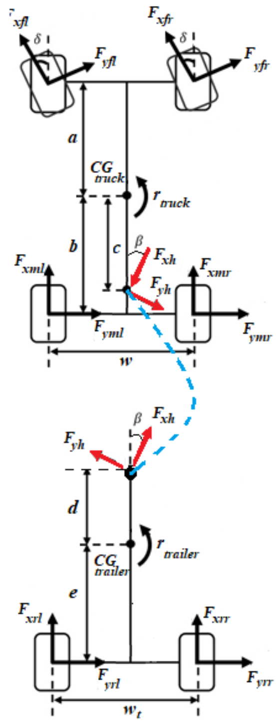

Next, the mathematical equations for the trailer handling model are as follows.

$$m_{trailer} a_{x2} = \left[F_{xrr} + F_{xrl} + F_{xh} \cos\beta + F_{yh} \sin\beta \right] \tag{14}$$

$$m_{trailer} a_{y2} = \left[F_{yrr} + F_{yrl} + F_{xh} \sin\beta - F_{yh} \cos\beta \right] \tag{15}$$

$$I_{ztrailer} \ddot{r}_{trailer} = \left[\frac{w_t}{2} F_{xrr} - \frac{w_t}{2} F_{xrl} + eF_{yrr} + eF_{yrl} - dF_{xh} \sin\beta + dF_{yh} \cos\beta \right] \tag{16}$$

where

$m_{trailer}$ = Mass of the trailer

$I_{ztrailer}$ = Yaw inertia of the trailer

d = Distance from the CG to the hitch

e = Distance from the CG to the trailer wheels

In this study, Calspan tyre model is used for the truck and trailer models in order to generate tyre forces in lateral and longitudinal directions. Calspan tyre model is more suitable for this study compared to others linear tyre model because linear tyre model does not consider tyre force in longitudinal due to extreme cornering conditions. The linear tyre model is more suitable to analyse a stable vehicle behaviour with small steering angle. The use of Calspan tyre model in this study is due to its capability to describe the exact full vehicle behaviours in any driving tests in various steering, speed and braking inputs (Adnan et al., 2020). All the parameters used in the modelling process are obtained from the TruckSim software as tabulated in Table 1.

Table 1 Single-trailer truck model parameters

Symbol	*Description*	*Value* (SI Unit)
I_{ztruck}	Truck yaw inertia	38403 kg.m^2
$I_{ztrailer}$	Trailer yaw inertia	54000 kg.m^2
I_{roll1}	Truck roll inertia	22839 kg.m^2
I_{roll2}	Trailer roll inertia	38140 kg.m^2
I_{pitch1}	Truck pitch inertia	35403 kg.m^2
I_{pitch2}	Trailer pitch inertia	41801 kg.m^2
m_{truck}	Truck mass	4455 kg
$m_{trailer}$	Trailer mass	6000 kg
h_{CG1}	CG height	2.39 m
a	Length from the front tyres to the truck CG	1.11 m
b	Length from the rear tyres to the truck CG	2.79 m
c	Length from the CG to the hitch	1.00 m
d	Length from the trailer CG to the hitch	5.22 m
e	Length from the CG to the trailer tyres	4.78 m
w	Truck width	2.44 m
w_t	Trailer width	2.44 m

2.2 Modelling of hitch joint using differential equation

The hitch joint links the truck and the trailer when travelling. The differential equations used in the hitch modelling give the lateral and longitudinal forces acting on the hitch joint (Adnan et al., 2020). The hitch joint longitudinal force (F_{xh}) is dependent on the truck response in the longitudinal direction (x,v_x and a_x) and yaw motion (r, $\dot{r}$ and $\ddot{r}$). Each term is associated with a constant value that has to be tuned to correspond with the trailer response. Therefore, the longitudinal force acting on the hitch is as follows.

$$F_{xh} = \left(a_1 x + a_2 v_x + a_3 a_x\right) + \left(a_4 r + a_5 \dot{r} + a_6 \ddot{r}\right) \tag{17}$$

The lateral force (F_{yh}) on the hitch is dependent on the steering action induced from the driver inputs namely angular acceleration ($\ddot{\delta}$), velocity ($\dot{\delta}$) and position (δ) of the steering wheel, and using the similar yaw truck response in calculating the F_{xh}. The equation for F_{yh} is calculated as shown below:

$$F_{yh} = \left(b_1\delta + b_2\dot{\delta} + b_3\ddot{\delta}\right) + (b_4 r + b_5\dot{r} + b_6\ddot{r}) \tag{18}$$

Meanwhile, the hitch angle (β) is calculated using the differential equation for the truck's lateral responses (y, v_y and a_y) and yaw responses (r, $\dot{r}$ and $\ddot{r}$).

$$\beta = \left(c_1 y + c_2 v_y + c_3 a_y\right) + (c_4 r + c_5\dot{r} + c_6\ddot{r}) \tag{19}$$

Here, a_1, a_2, a_3, a_4, a_5, a_6, b_1, b_2, b_3, b_4, b_5, b_6, c_1, c_2, c_3, c_4, c_5 and c_6 are the constants that need to be tuned to obtain the accurate hitch model.

Finally, all the equations for each subsystem are then developed in Matlab and merged to form a full 18-DOF single-trailer truck model as shown in Figure 4 which consists of ride, handling and tyre for truck and trailer subsystems, respectively as well as hitch joint subsystem. The input for the single-trailer truck model is the steering wheel angle from the driver which is used mainly for truck handling model and tyre slip equation. Each handling model for truck and trailer will determine the accelerations in lateral and longitudinal directions, and yaw rate based on the input obtained from the driver. Beside that a few forces generated from hitch and tyre model also used as the inputs for the handling models. These outputs from handling model are then fed into tyre slips equation to estimate the lateral slip angle. The lateral slip angle for each value is then forwarded into tyre model to estimate lateral tyre force and longitudinal tyre force. These forces are to be fed back into the handling model as main input. The tyre model also receives vertical tyre force as input which were obtained from ride model. Ride model is developed by considering forces and moments in vertical plane and thus, producing overall vertical forces based on lateral force response from the handling model.

Figure 4 Single-trailer truck vehicle model simulated in Matlab/SIMULINK (see online version for colours)

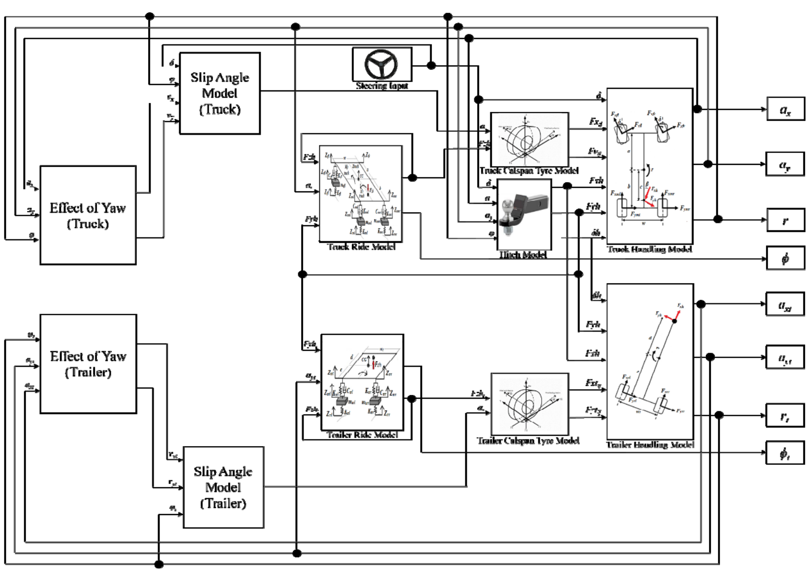

3 Development of active roll control for single-trailer truck using steerable-wheel at middle axle

Steerable-wheel (SW) system at middle axle as an ARC in this study is using a pitman arm mechanism system as shown in Figure 5. This type of mechanism is commonly known for heavy-duty applications (Aparow et al., 2016). Here, the SW system using pitman arm system is designed to provide several advantages for the single-trailer truck such as the capability to deliver a sufficient wheel angle in rejecting the unwanted motions of trailer due to steering input from driver and stabilising the direction of the vehicle after lane change manoeuvre.

Figure 5 Steerable middle wheel of the middle axle for single-trailer truck (see online version for colours)

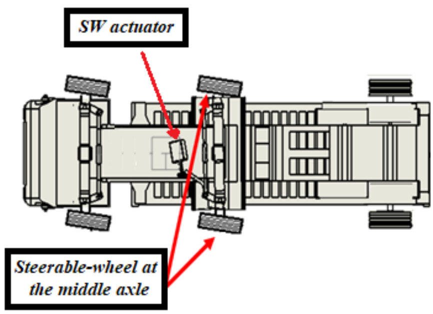

Figure 6 Control structure of ARC using SW at the middle axle (see online version for colours)

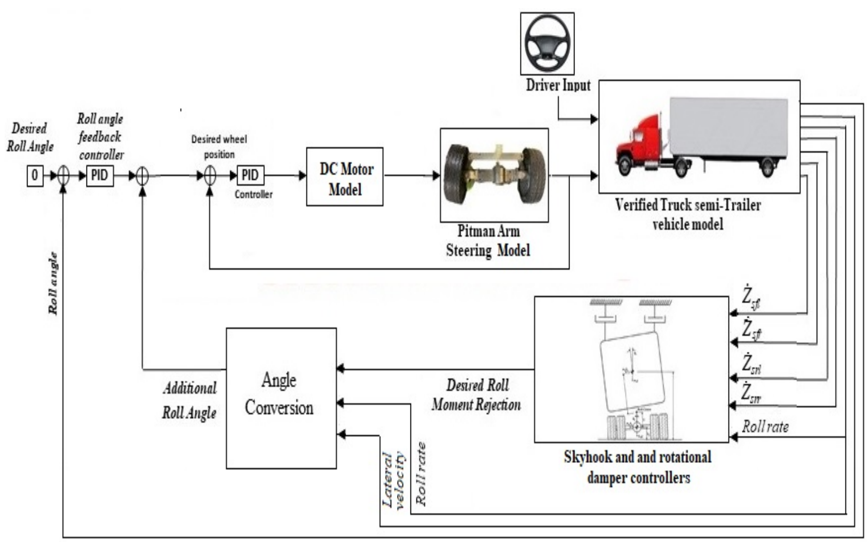

In this section, a control structure for ARC using SW at the middle axle to be used in single-trailer truck is constructed based on the verified 18-DOF model. The control structure is based on inner-loop and outer-loop controller feedbacks as illustrated in Figure 6. Inner loop controller feedback is used to actuate the SW mechanism using a DC motor as set in the outer loop controller, where it is designed to minimise the unwanted motions of trailer during manoeuvring using PID merged with skyhook controller. This provides a roll control in reducing the unwanted roll angle, yaw rate and lateral acceleration of trailer body so that can minimise the load transfer during cornering manoeuvres.

In outer loop controller, there is an additional roll moment cancellation controller to calculate the additional rejection angle of trailer roll (ϕ_{add}) due to load transfer. It is constructed based on four units of skyhook damper installed at each corner of trailer and a rotational damper at the trailer CG as shown in Figure 7.

Figure 7 Additional controller for outer loop feedback: (a) skyhook damper at each corner of trailer and (b) rotational damper at trailer CG (see online version for colours)

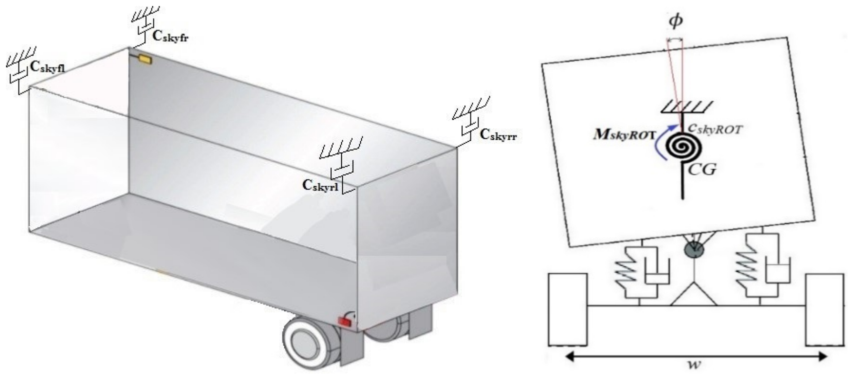

(a) (b)

These imaginary dampers are used to dissipate any unwanted load transfer of trailer into overall control system. The skyhook control policy is given as (Nie et al., 2017; Chen et al., 2020; Papaioannou et al., 2021; Rahmat et al., 2021):

$$F_{sky_{ij}} = -C_{sky_{ij}} \dot{Z}_{s_{ij}} \tag{20}$$

The skyhook forces (F_{sky}) at each corner of trailer are then used to calculate the ideal desired moment to reject the unwanted roll motion by converting it into a rotating skyhook moment (M_{skyij}) at the CG of the trailer body (Aparow et al., 2016). Next, the total M_{skyij} generated from the skyhook force is merged with a rotating skyhook damper at trailer CG to calculate the additional roll moment (M_{roll}) for the overall control structure as follow:

$$\sum M_{roll} = M_{sky_{fl}} + M_{sky_{fr}} + M_{sky_{rl}} + M_{sky_{rr}} + M_{skyROT} \tag{21}$$

where

$M_{sky_{fl}} = F_{sky_{fl}} \left(\frac{w}{2}\right) = -C_{sky_{fl}} \dot{Z}_{s_{fl}} \left(\frac{w}{2}\right) =$ skyhook moment at the front-left corner

$M_{sky_{fr}} = F_{sky_{fr}} \left(\frac{w}{2}\right) = -C_{sky_{fr}} \dot{Z}_{s_{fr}} \left(\frac{w}{2}\right) =$ skyhook moment at the front-right corner

$M_{sky_{rl}} = F_{sky_{rl}} \left(\frac{w}{2}\right) = -C_{sky_{rl}} \dot{Z}_{s_{rl}} \left(\frac{w}{2}\right) =$ skyhook moment at the rear-left corner

$M_{sky_{rr}} = F_{sky_{rr}} \left(\frac{w}{2}\right) = -C_{sky_{rr}} \dot{Z}_{s_{rr}} \left(\frac{w}{2}\right) =$ skyhook moment at the rear-right corner

$M_{skyROT} = C_{skyROT}\dot{\phi}$ = rotating skyhook moment at the trailer centre of gravity

Finally, an additional rejection angle of trailer roll that processed by the addition roll moment cancellation controller need to be calculated in order to merge it with the outer loop controller of ARC. Here, the total additional moment obtained in equation (22) is then converted into the additional rejection angle of roll as follow:

$$\phi_{add} = \frac{\left(k_1 \sum M_{roll} - k_2\dot{\phi} - k_3 v_y\right)}{i} \tag{22}$$

where $\dot{\phi}$ is the roll rate and v_y is the lateral velocity of the trailer. Meanwhile, k_1, k_2 and k_3 are the conversion gains for roll moment, roll rate and lateral velocity, respectively in calculating the additional roll angle (ϕ_{add}), and finally i is tunable to obtain a better trailer response as well as the skyhook controller parameters are presented in Table 2.

Table 2 Skyhook controller parameters

Skyhook controller	*Symbols*	*Value* (Ns/m)
Skyhook (*front right*)	C_{skyFL}	2.5
Skyhook (*front left*)	C_{skyFR}	3.5
Skyhook (*rear right*)	C_{skyRL}	1
Skyhook (*rear left*)	C_{skyRR}	1
Rotating Skyhook	C_{skyROT}	–0.1

4 Simulation results of active roll control using steerable-wheel at the middle axle for single-trailer truck

After developing the control structure of ARC using PID-skyhook controller, the performance is then simulated in Matlab software by comparing its responses against the passive system and ARC using PID. The purpose of designing the PID-skyhook controller is to further improve the performance of ARC control structure by reducing the magnitude of unwanted motions in terms root-mean-square (RMS) values of lateral acceleration, yaw rate and roll angle of the trailer as well as rearward amplification ratio (RWA). The 15 s simulation time is set to simulate the SW system at middle axle in stabilising the single-trailer truck model with two type of manoeuvring tests namely SLC and DLC at cruising speeds of 60 km/h and 80 km/h with steering wheel angles as illustrated in Figure 8, respectively.

Figure 8 Steering wheel angles for SLC and DLC manoeuvres at 60 km/h and 80 km/h: (a) SLC at 60 km/h; (b) SLC at 80 km/h; (c) DLC at 60 km/h and (d) DLC at 80 km/h

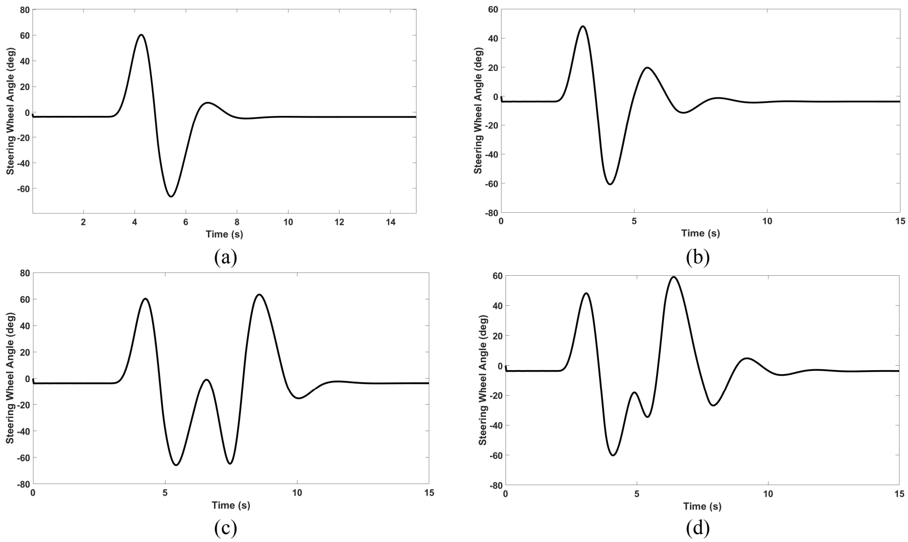

SLC and DLC are considered in this study is due to observe the manoeuvrability of single-trailer truck in extreme driving condition. Realistically, SLC and DLC cause a roll motion resulting in discomfort and load transfer in lateral direction as well as causing tyres to lose contact with the road surface. This contributes to the instability of handling performance of the single-trailer truck in which leads to rollover accident.

4.1 Simulation results of the proposed ARC control structure during single lane change

Figures 9–11 show the responses for SLC at 60 km/h and 80 km/h in terms of lateral acceleration, yaw rate and roll angle. Based on the lateral acceleration results obtained in Figure 9(a) and (b) for both speeds, it can be seen that there is a slight improvement of PID-skyhook in reducing the unwanted lateral acceleration as compared to PID and better reduction against the passive system. The percentages of improvement recorded for both speeds in terms of RMS for PID-skyhook are 28.85% at 60 km/h and 6.56% at 80 km/h as compared to passive system. Better performance of single-trailer truck's rotational motion can be observed by analysing the yaw rate response for both PID-skyhook and PID controllers. Figure 10(a) and (b) show the yaw rate responses at the trailer CG are 60 km/h and 80 km/h, respectively. Similar to the lateral acceleration response, PID-skyhook and PID controllers show the capability in dropping the magnitude of yaw rate response against the passive system. However, by referring to the percentage of improvement in terms of RMS value, it can be seen that PID-skyhook controller provides better rejection control about 28.61% at 60 km/h and 6.87% at 80 km/h. Meanwhile, 27.78% and 4.94% reductions are recorded for PID controller at both speeds 60 km/h and 80 km/h, respectively.

Figure 9 Lateral acceleration responses for SLC test: (a) 60 km/h and (b) 80 km/h

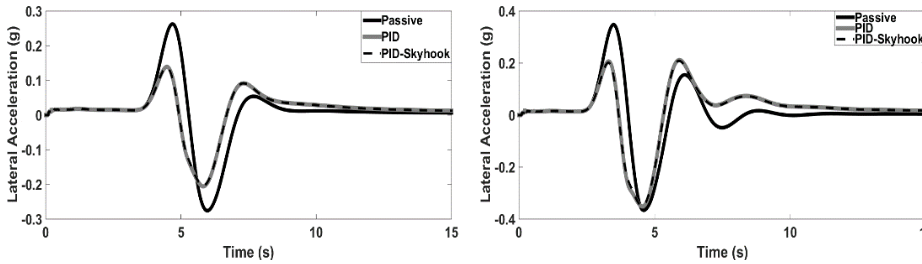

(a) (b)

Figure 10 Yaw rate responses for SLC test: (a) 60 km/h and (b) 80 km/h

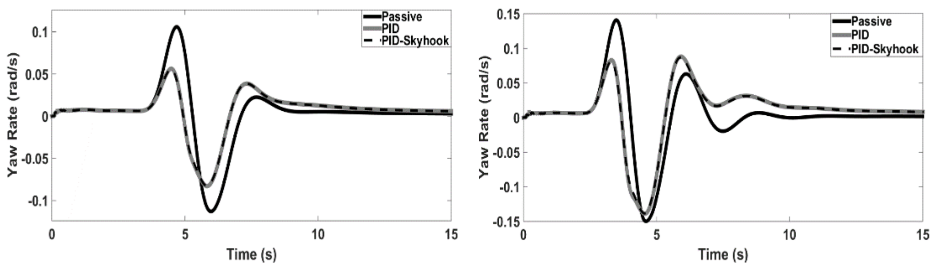

(a) (b)

Figure 11 Roll angle responses for SLC test: (a) 60 km/h and (b) 80 km/h

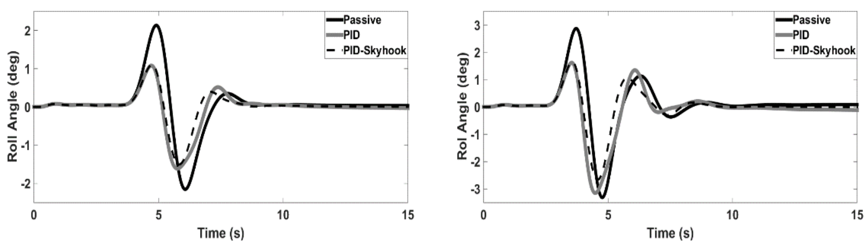

(a) (b)

When observing the roll angle response as presented in Figure 11 for both speeds, it can be seen that the PID-skyhook controller performs significantly better in reducing the magnitude compared to its counterparts namely PID controller and passive system. The better performance was mainly due to the ARC with PID-skyhook controller, which was designed to be able to reject the roll motion. Also, involvement of additional roll moment cancellation loop consists of imaginary damper at each corner and rotary damper at CG of the trailer body to provide sudden load transfer to the ARC control structure, which contributes to the overall achievement of the proposed system. The performance improvement is noticeable after 5 s during the driver drives the truck in straight direction, where the SW manages to reduce the magnitude and followed with the faster time response in stabilising the trailer than PID controller. The percentages of improvement in terms of RMS value for PID-skyhook against passive system for both speeds are 39.33% and 27.01% at the speeds of 60 km/h and 80 km/h, respectively. Overall improvements for SLC tests for both speeds against the passive system are tabulated in Table 3.

Table 3 Percentage of improvement responses based on RMS for SLC test

Case	*Response*	*Speed* (km/h)	*Root mean square (RMS)* *Passive*	*PID*	*PID-Skyhook*	*Improvement percentage (%)* *PID*	*PID-Skyhook*
SLC	Lateral acceleration	60	0.0884	0.0636	0.0629	28.05	28.85
		80	0.1144	0.1093	0.1069	4.46	6.56
	Yaw rate	60	0.036	0.026	0.0257	27.78	28.61
		80	0.0466	0.0443	0.0434	4.94	6.87
	Roll angle	60	0.6547	0.4563	0.3972	30.30	39.33
		80	0.912	0.8152	0.6657	10.61	27.01

In order to evaluate the roll stability of the proposed ARC for single-trailer truck, a RWA is used as proposed by Ervin and Guy (1986). The RWA is a phenomenon where the trailer tends to over-respond in lateral direction during manoeuvrings (Chen et al., 2019). Figure 12 shows the RWA values for various combination type of truck vehicles where it is defined as the ratio of the peak value of lateral acceleration between the rearmost trailer and the truck at its CG (Wang and He, 2016; Chen et al., 2019). The lower value of RWA ratio provides better ride of truck and less tendency to rollover. RWA is calculated as follows:

$$Rearward\ Amplification\ Ratio\left(RWA\right) = \frac{Peak(a_{y_{rearmost.trailer}})}{Peak(a_{y_{truck}})} \tag{23}$$

Table 4 shows the RWA ratio of the single-trailer truck during SLC manoeuvre at 60 km/h and 80 km/h. Based on the RWA ratio results, the ARC with PID controller provides less RWA value compared to the passive system at both speeds. However, the ARC with PID-Skyhook shows the lowest RWA ratio at both 60 km/h and 80 km/h speeds, 1.1012 and 1.0571 respectively against the ARC with PID.

Figure 12 Rearward amplification affects the combination heavy vehicles

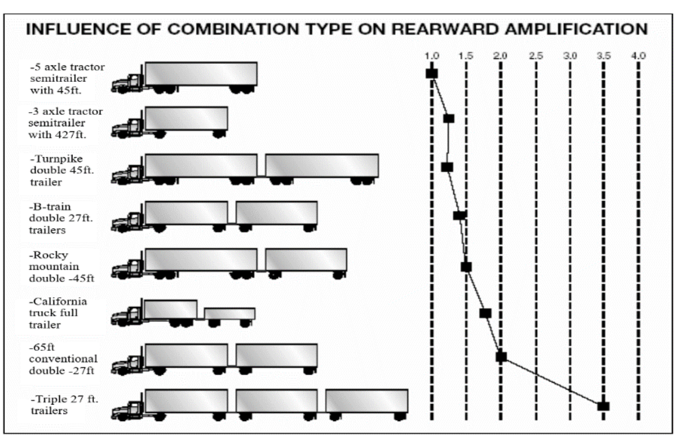

Source: Ervin (1983)

Table 4 RWA ratio by trailer towards truck for SLC test

Case	*Speed* (km/h)	*Peak a_y* (g)		*RWA ratio*
		Truck	*Trailer*	
Passive	60	0.190	0.264	1.3842
	80	0.260	0.350	1.3462
PID	60	0.110	0.139	1.2636
	80	0.180	0.200	1.1111
PID-Skyhook	60	0.168	0.185	1.1012
	80	0.140	0.148	1.0571

4.2 *Simulation results of the proposed ARC control structure during double lane change*

Next manoeuvring assessment is DLC test for speeds of 60 km/h and 80 km/h. For both lateral acceleration and yaw rate responses as presented Figures 13 and 14, the ARC with PID-skyhook and ARC with PID have better performance than the single-trailer truck without SW system in terms of the magnitude reduction. It indicates that the ARC using SW system has the ability to reduce both unwanted acceleration and yaw rate due to the steering input from driver. However, ARC with PID-skyhook controller has a slight RMS percentage of improvement against the ARC with PID at both speeds 60 km/h and 80 km/h which are 38.03% and 25.32% for lateral acceleration, and 37.8% and 25.81% for yaw rate, respectively. Meanwhile, 37.47% and 23.32% of lateral acceleration, as well as 37.2% and 24.19% of yaw rate were recorded as compared to RMS of passive system for both 60 km/h and 80 km/h. Here, it can be seen that there is a minor contribution of additional roll moment cancellation controller in enhancing mobility of the truck.

Figure 13 Lateral acceleration responses for DLC: (a) 60 km/h and (b) 80 km/h

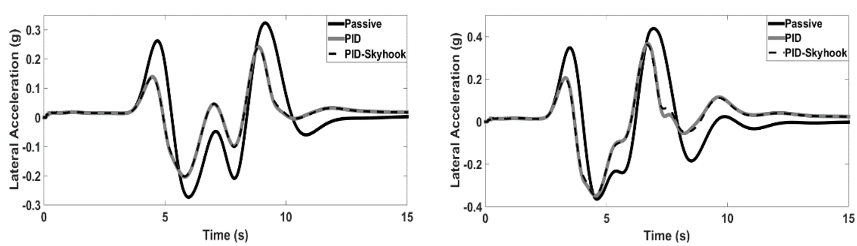

(a) (b)

Figure 14 Yaw rate responses for DLC: (a) 60 km/h and (b) 80 km/h

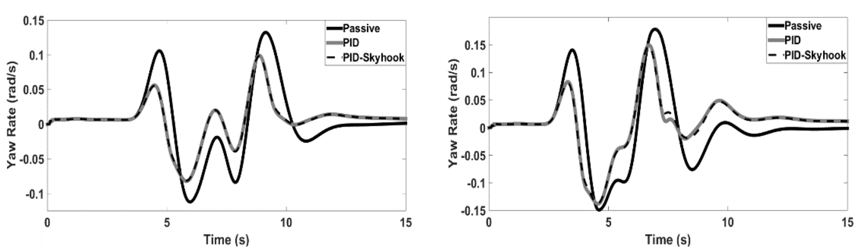

(a) (b)

A notable improvement of the proposed controller of ARC can be noticed from the roll angle responses as shown in Figure 15 for both speeds. Here, the yaw angle responses of the ARC with PID-skyhook and ARC with PID are compared to passive truck. By observing the percentage of improvement in RMS values, it can be noted that that the roll angle response for ARC with PID in DLC test managed to reduce the unwanted roll motion by 34.72% and 22.86% for respective cruising speed. Additionally, the roll angle response for the ARC with PID-Skyhook also denotes better roll motion performance as compared to ARC with PID by reducing the roll angle by 37.08% and 32.46% at 60 km/h and 80 km/h, respectively. Since the roll motion of the ARC with PID-skyhook controller shows a slight improvement, the possibility of the developed ARC with PID-skyhook control structure in enhancing the dynamics stability of the single-trailer truck during extreme manoeuvring to avoid rollover accident is promising. The RMS values of the lateral, yaw and roll motions for passive, ARC with PID and ARC with PID-skyhook are demonstrated in Table 5.

Figure 15 Roll angle responses for DLC: (a) 60 km/h and (b) 80 km/h

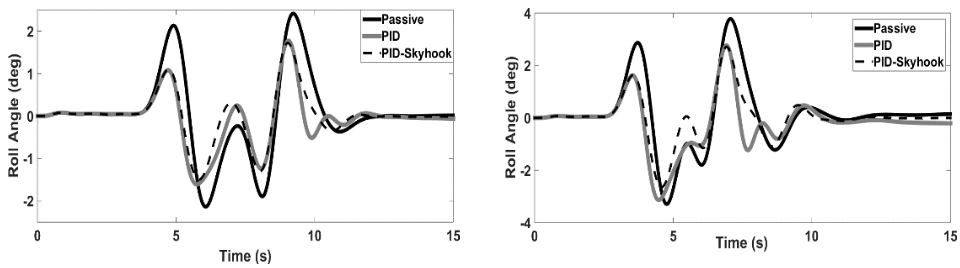

(a) (b)

Table 5 Percentage of improvement responses based on RMS

			Root mean square (RMS)			*Improvement percentage (%)*	
Case	*Response*	*Speed* (km/h)	*Passive*	*PID*	*PID-Skyhook*	*PID*	*PID-Skyhook*
DLC	Lateral acceleration	60	0.1249	0.0781	0.0774	37.47	38.03
		80	0.1663	0.1268	0.1242	23.75	25.32
	Yaw rate	60	0.0508	0.0319	0.0316	37.20	37.8
		80	0.0678	0.0514	0.0503	24.19	25.81
	Roll angle	60	0.9247	0.6063	0.5818	34.72	37.08
		80	1.2762	0.9872	0.8619	22.864	32.46

Next, RWA ratio of single-trailer truck during DLC test is shown in Table 6. The passive system during DLC test at 60 km/h has RWA ratio of 1.3684. The RWA ratio is successfully reduced to 1.2727 using ARC with PID controller. However, the RWA ratio shows the lowest value ARC with PID-Skyhook controller, which is 1.0952. Similar improvement also can be observed for DLC test at 80 km/h, where a significant improvement with a reduction of RWA ratio from 1.4313 for passive system to 1.1389 for ARC with PID-Skyhook.

Table 6 RWA ratio by trailer towards truck for DLC test

Case	*Speed* (km/h)	*Peak* a_y (g)		*RWA ratio*
		Truck	*Trailer*	
Passive	60	0.19	0.26	1.3684
	80	0.255	0.365	1.4313
PID	60	0.11	0.14	1.2727
	80	0.179	0.206	1.1508
PID-Skyhook	60	0.168	0.184	1.0952
	80	0.18	0.205	1.1389

The effectiveness of ARC using SW at the middle axle which consists of PID-skyhook controller has been successfully simulated based on 18-DOF single-trailer truck model. The purpose of the developed control structure is to improve the handling performances mainly focused on lateral acceleration, yaw rate and roll angle during manoeuvring. From the simulation results, a better handling performance can be observed in terms of reducing the unwanted motions in preventing the single-trailer truck from rollover. Next, the modelling assumptions and parameters used in single-trailer truck as well as the validity of controller development theories will be tested experimentally using HiLS in the next section.

5 Hardware-in-the-loop simulation (HiLS) of steerable-wheel actuator

Figure 16 shows the experimental setup of HiLS for steerable-wheel (SW) actuator which consists of hardware and software configurations. The software configuration includes the xPC Target linked with Matlab and signal interface between host PC to target PC. Meanwhile, steerable-wheel for middle axle system, steerable-wheel actuator, angle sensors to record the wheel angle position, DAQ, target PC, host PC with Matlab, network cable, power supply, and pin out board for actuator and angle sensor connection are used as the hardware configuration.

Figure 17 illustrates the process of HiLS testing using test rig equipped with the SW actuator implemented at middle axle for single-trailer truck. For HiLS testing, the system configuration is focused on both software and hardware configurations. In terms of software configuration, Matlab Simulink is used as the platform to configure the controller design. A conventional PID controller is used to provide current output for the DC motor and rotational switching which will be used as the input for the National Instrument (NI) analogue output block namely PCI-6229. The analogue output block is mainly used to convert the digital output into analogue input which will be connected to the National Instrument data acquisition system (DAQ). The DAQ is connected with motor driver in order to amplify the voltage required by the SW actuator, which is 12 V. Other than that, the motor driver is also used to provide the rotational switching either in forward or reverse direction based on the PID controller output. Since the SW actuator is connected at the middle axle for single-trailer truck, an angle sensor is required to measure the rotational angle in z-direction. The output measured from the angle sensor is feedback to the DAQ before connecting to the Matlab Simulink. The output from DAQ is connected with PCI-6229 National Instrument (NI) analogue input block to convert the analogue outputs from angle sensor as digital input. This digital input is calibrated using analogue filter to reduce the unwanted noise during testing. The filter digital input is fed back as actual angle to the comparator block. The results processed in HiLS are compared with the results obtained from the developed model in Matlab to verify the position tracking control capability of the SW actuator.

Figure 16 HiLS setup for SW actuator (see online version for colours)

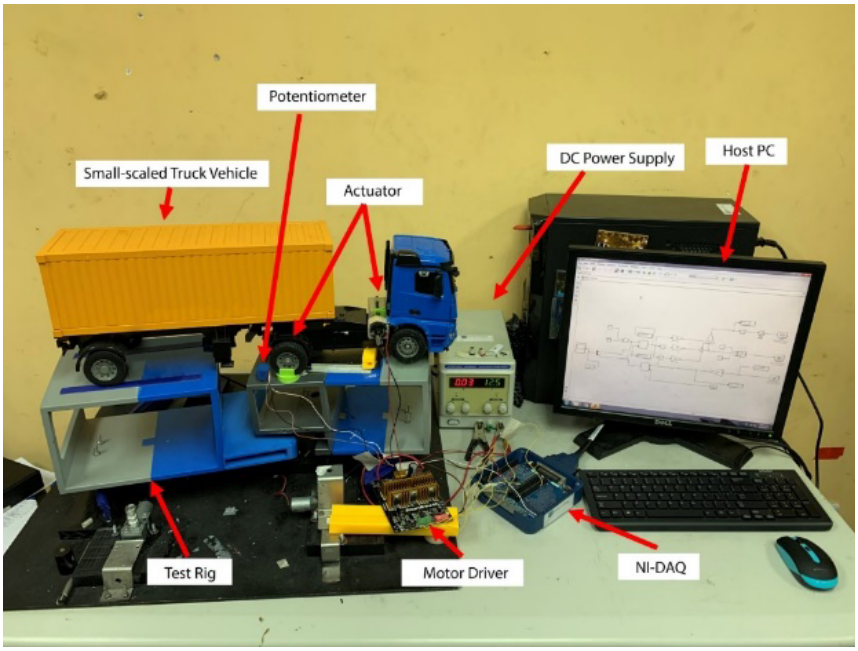

Figure 17 HiLS process for SW actuator (see online version for colours)

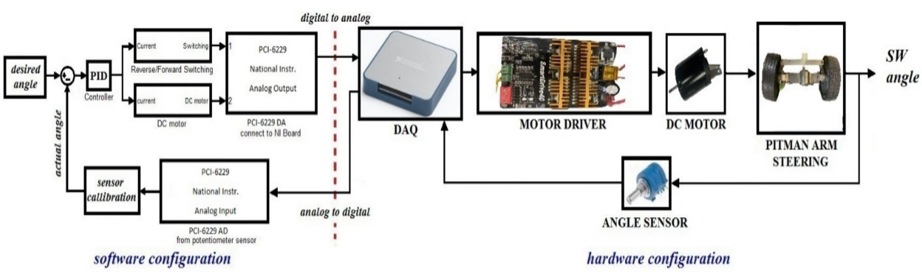

There are two input command functions namely square and sine inputs, with a frequency of 0.25 Hz implemented for this position tracking control of SW actuator. In order to investigate the capability of the developed SW in tracking the targeted input command, its actuator is evaluated in simulation approach using Matlab-Simulink and experimental test via HiLS. Here, both simulation and experiment are performed for a period of 20 s with the targeted steer angle of 3 deg. Table 7 illustrates the PID controller parameters used in simulation and experiment. From the PID controller parameters, it can be seen that the parameters implemented in experiment are higher against the simulation because of the few factors namely delay in tracking response due to connection mechanism between actuator and middle axle of the truck as well as friction between wheel surface and test rig platform. In order to evaluate the effectiveness of the actuator, its response in tracking the angle set in the controller command is evaluated in terms of RMS error.

Table 7 Controller parameters used in simulation and HILS

Techniques	*P*	*I*	*D*
Simulation	1	0	0.1
HiLS	44	54	1

Figure 18 indicates the position tracking responses for square and sine input functions. It can be seen from the results of simulation response that the developed actuator model is able to follow well the targeted angle with minor percentage of RMS error which are about 4.9% and 1.1% compared to the targeted angle for square and sine function, respectively. As compared to experimental response obtained from HiLS test, the results show that the percentage of error are slightly increase with acceptable range about 14.1% for square and 0.8% for sine compared to targeted angle. In addition, experimental result using HiLS also indicates the time delay for both square and sine inputs which are 0.25 s and 0.32 s, respectively. The factors that lead to delay are due to the backlash motion of the gear set between SW actuator and axle as well as the connection of angle sensor. Overall the percentage of RMS error against the targeted angle are for both simulation and experiment using HiLS as tabulated in Table 8.

Figure 18 The position tracking responses for the square and sine input functions: (a) square function and (b) sine function

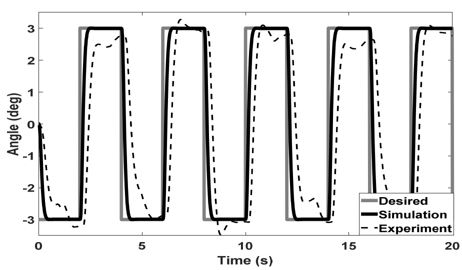

(a)

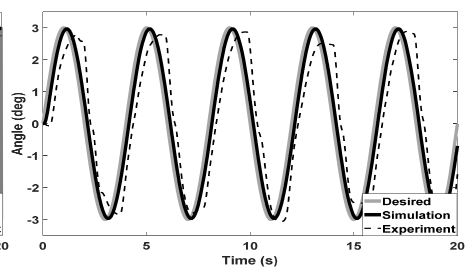

(b)

Table 8 Overall percentage of RMS error of the simulation and experiment relative to the target angle

Inputs	*RMS values*			*Error percentage (%)*	
	Desired	*Simulation*	*Experiment*	*Simulation*	*Experiment*
Square	3.00	2.85	2.58	4.9	14.1
Sine	2.12	2.09	2.10	1.1	0.8

6 Experimental results of the proposed control structure for active roll control using hardware-in-the-loop simulation

After designing the working principle of control structure for ARC, the performance of the proposed controller is tested experimentally using real-time approach through HiLS to validate the concept of the SW at the middle axle for single-trailer truck as shown in Figure 19. The working principle of SW in HiLS for the single-trailer truck is: the outer controller output in simulation is linked to the actuator SW driver to produce the appropriate wheel angle. The wheel angle at the middle axle is observed using the angle sensor and next used as the feedback for the SW actuator controller command through xPC Target in Target PC. The SW angle is also used as controller input in reducing the truck motions namely roll angle, lateral acceleration and yaw rate which will be analysed in the HiLS testing. In order to validate the SW, the experimental results from HiLS are compared against the desired angle set in the simulation based on the control structure of ARC. Here, the accuracy in terms of formulation approach of the controller as well as the selection process of single-truck trailer parameters that used in the model development can be verified.

Figure 19 HiLS process to validate the ARC model that uses an SW at the middle axle (see online version for colours)

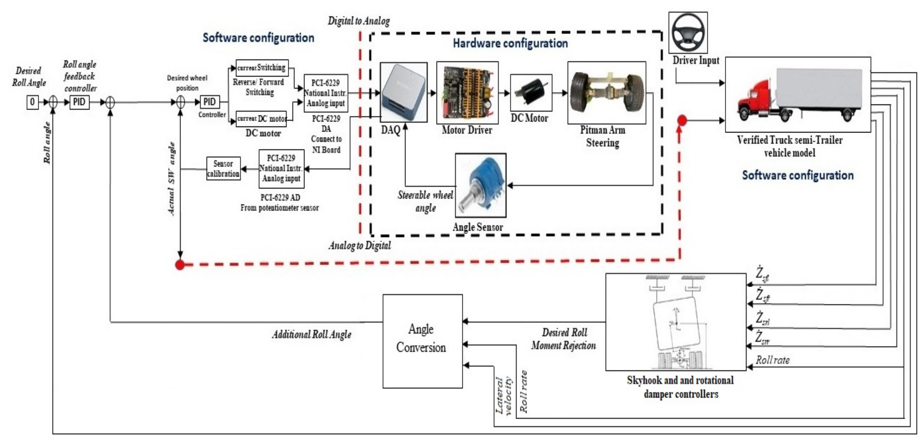

Experimental test via HiLS is performed through simulation environment namely Matlab-Simulink for the SLC and DLC manoeuvres at constant speeds of 60 km/h and 80 km/h. The two manoeuvre tests with different speed are considered in this study and are used to observe the benefits of the developed system in various driving conditions. Here, four single-trailer truck responses are investigated namely the position tracking control of wheel angle at the middle axle, yaw rate, roll angle and lateral acceleration. All these responses obtained from the experimental test are compared against the developed control structure to assess the SW actuator in delivering the middle axle wheel angle and next enhance the roll stability of single-trailer truck.

6.1 *Experimental results of ARC control structure for single lane change at 60 km/h and 80 km/h*

The performances of the proposed ARC at 60 km/h for SLC test are demonstrated in Figure 20(a)–(d). In terms of position tracking control of SW actuator at the middle axle, the simulated SW angle obtained from the control structure is set as the targeted angle for the single-trailer truck. Here, targeted angle must be tracked by the SW actuator to reduce the magnitude of the single-trailer truck response namely roll angle, yaw rate and lateral acceleration during manoeuvring. In order to evaluate the capability of the actuator, actual SW angle is recorded from the actual system in the HiLS test rig. It can be seen that the result of actual SW system taken from HiLS managed to track the actual steer angle of the middle axle with similar trend and slight time delay with percentage of RMS error 0.31% against the simulated result as illustrated in Figure 20(a). Further observation on the trailer responses in HiLS namely lateral acceleration, yaw rate and roll angle in Figure 20(b)–(d), clearly shows that a good agreement can be found as compared to the simulated responses obtained from the control structure with percentage of RMS error less than 6% for all responses in which can be considered within the acceptable range of error in experimental works.

Figure 20 The performance of the proposed ARC for SLC at 60 km/h: (a) wheel angle of SW; (b) lateral acceleration; (c) yaw rate and (d) roll angle

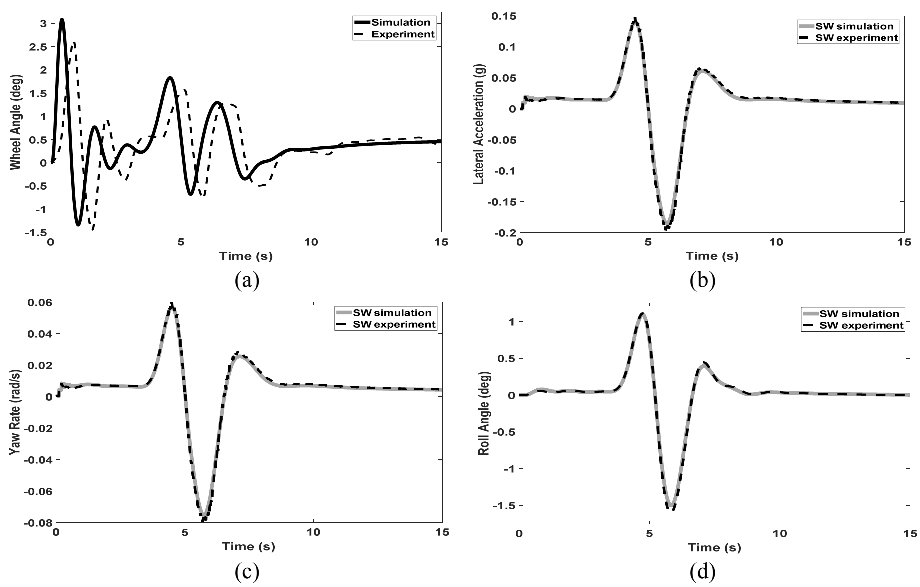

Next, the responses of SLC test at 80 km/h of SW system for ARC in single-truck trailer are presented in Figure 21. Figure 21(a) presents the performance of position tracking control for the SW system. For 80 km/h test, a smaller steer angle for SW system is required as compared to 60 km/h test to prevent the vehicle from roll. It is due to the fact that the capability of SW to provide a fast response in higher speed manoeuvring to track the path of SLC manoeuvre as set in the controller. It is also observed that the SW is able to provide the actual wheel angle at the middle axle in similar trend with minor time delay of 5% as in the simulated angle. Next, the performance of the SW via HiLS in tracking the simulated responses namely lateral acceleration, yaw rate and roll angle are presented in Figure 21(b)–(d). From the all responses, it can be seen that all the experimental responses obtained throughout the HiLS are able to produce similar responses with less than 5% of RMS error against simulation as tabulated in Table 9.

Figure 21 The performance of the proposed ARC for SLC at 80 km/h: (a) wheel angle of SW; (b) lateral acceleration; (c) yaw rate and (d) roll angle

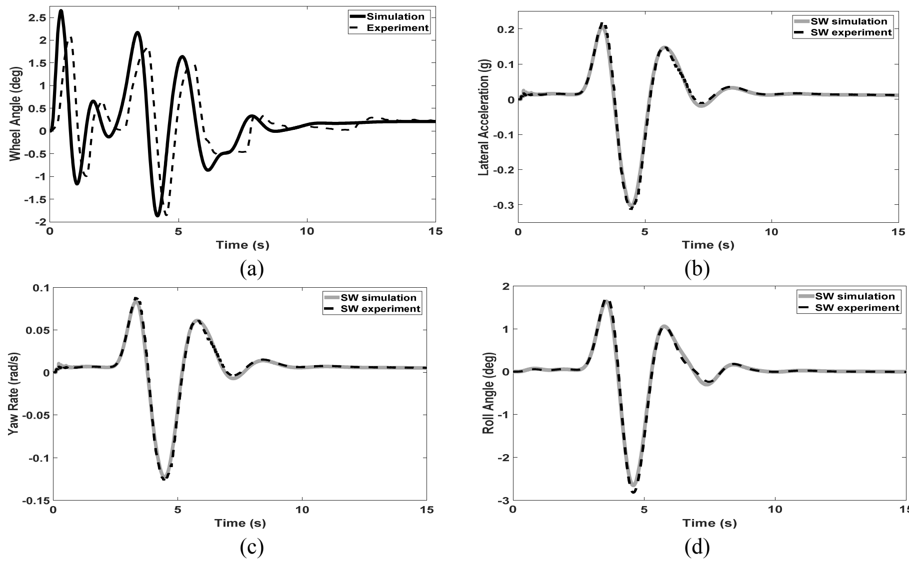

Table 9 Overall difference percentage of the RMS for the proposed ARC with SW in the SLC test with HiLS

Test	Response	*Speed* (km/h)	*RMS*		*Difference percentage* (%)
			Simulation	*Experiment*	
SLC	SW angle	60	0.7447	0.7470	0.31
		80	0.7707	0.6924	10.16
	Lateral acceleration	60	0.0531	0.0560	5.46
		80	0.0844	0.0873	3.44
	Yaw Rate	60	0.0217	0.0229	5.53
		80	0.0344	0.0356	3.49
	Roll Angle	60	0.3968	0.4194	5.69
		80	0.6645	0.6943	4.48

6.2 *Experimental results of ARC control structure for double lane change at 60 km/h and 80 km/h*

Next rollover assessment of the proposed ARC system is DLC test in which this manoeuvre extremely evaluates the emergency handling performance of the single-trailer truck in avoiding an obstacle during driving. Figures 22(a) and 23(a) present the position tracking performance of the SW actuator at 60km/h and 80 km/h, respectively. Due to the extreme manoeuvre as compared to SLC test, the SW actuator is highly responsive in changing the direction of trailer in a short period of time to avoid a rollover accident. Here, it can be observed the SW actuator is able to produce required angle for both speeds as commanded by the controller in terms of the magnitude and the trend. However, 9.58% and 6.41% RMS errors are recorded with time delay of 0.4 s and 0.3 s for 60 km/h and 80 km/h, respectively.

Figure 22 The performance of the proposed ARC for DLC at 60 km/h: (a) wheel angle of SW and (b) lateral acceleration; (c) yaw rate and (d) roll angle

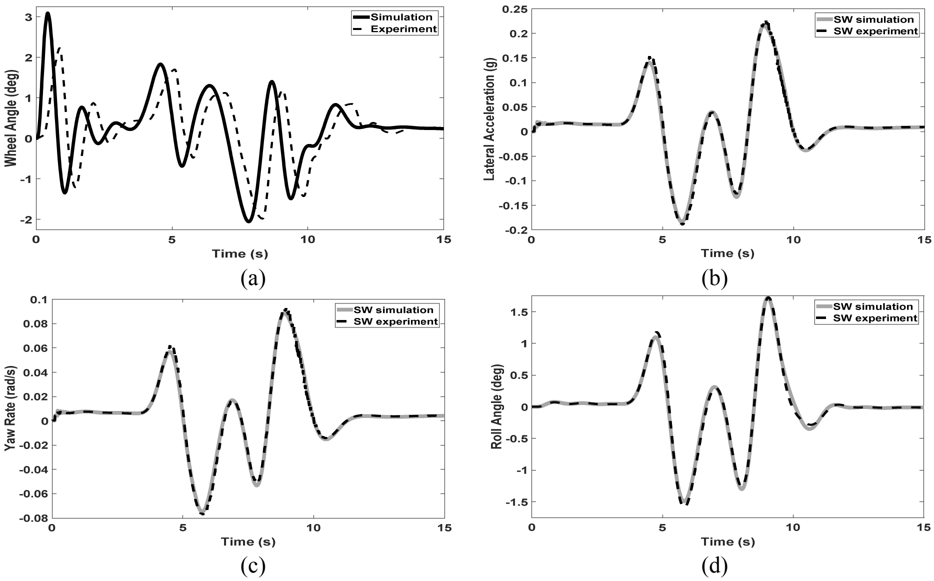

Figure 23 The performance of the proposed ARC for DLC at 80 km/h: (a) wheel angle of SW and (b) lateral acceleration; (c) yaw rate and (d) roll angle

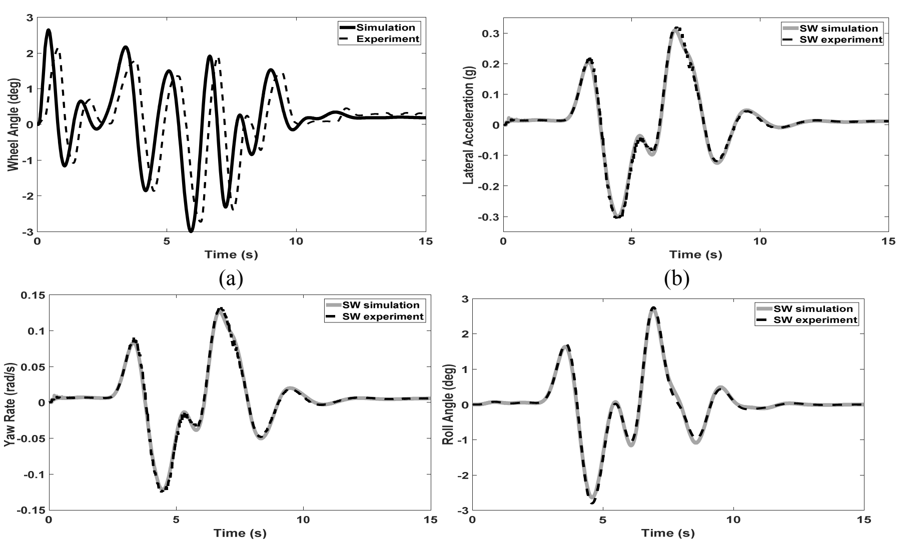

Comparisons between simulation of ARC control structure and its implementation using HiLS at both speeds 60 km/h and 80 km/h during DLC test are shown in Figures 22(b)–(d) and 23(b)–(d), respectively. All the assessment criteria namely lateral acceleration, yaw rate and roll angle for both speeds obtained from the HiLS results are also managed to track all responses as set in the controller with tolerable error. The highest RMS errors for DLC is recorded at 80 km/h which are lateral acceleration is 2.37%, yaw rate is 2.46% and roll angle is 2.64%. Meanwhile, lower RMS error which is less than 2% was also recorded for 60km/h in all responses as tabulated in Table 10.

Table 10 Overall difference percentage of RMS for the proposed ARC with SW tested with HiLS in a DLC manoeuvre

Test	*Response*	Speed (km/h)	*RMS*		*Difference percentage of RMS (%)*
			Simulation	*Experiment*	
DLC	SW angle	60	0.9027	0.8162	9.58
		80	1.0339	0.9676	6.41
	Lateral Acceleration	60	0.0758	0.0770	1.58
		80	0.1098	0.1124	2.37
	Yaw Rate	60	0.0310	0.0314	1.29
		80	0.0447	0.0458	2.46
	Roll Angle	60	0.5820	0.5929	1.87
		80	0.8611	0.8838	2.64

7 Conclusion

In order to enhance the roll stability of single-trailer truck, a control structure for ARC using steerable-wheel (SW) system at the middle axle was proposed. The proposed ARC was simulated based on verified 18-DOF model and its performance was compared against the passive system in two handling tests namely single SLC and DLC manoeuvres at 60 km/h and 80 km/h. The simulation results for both manoeuvres in two cruising speed 60 km/h and 80 km/h show better performance as compared to passive system in terms of lateral acceleration, yaw rate and roll angle. Here, the effectiveness of the ARC was proven to have a faster response in reducing the unwanted lateral, yaw and roll motions. The proposed ARC was then experimentally evaluated via HiLS test rig to verify the capability of the SW actuator in providing the middle axle angle as set in the controller. SW in HiLS test rig was developed, which consists of a DC motor, SW at middle axle, small-scaled single-trailer truck and test rig platform. From the HiLS test results, good agreement in terms of trend and magnitude within the acceptable range of error can be observed from the small-scaled system responses and simulated responses from the control structure in simulation works of ARC namely SW angle at the middle axle, lateral acceleration, yaw rate and roll angle. This proves the benefits of the proposed ARC using SW system at middle axle to be able to reduce and stabilise the yaw and lateral motions compared to the conventional system of a single-trailer truck.

Acknowledgement

The research has been carried out under Fundamental Research Grant Scheme project FRGS/1/2018/TK03/UPNM/03/2 provided by Ministry of Education of Malaysia

References

Adnan, M.N., Kadir, Z., Amer, N., Hudha, K., Yussof, M. and Aparow, V. (2020) 'Development and verification of a 3 – DoF trailer model for truck vehicles', *2020 16th IEEE International Colloquium on Signal Processing and Its Applications (CSPA)*, Langkawi, Malaysia, pp.120–125.

Ahmad, F., Hudha, K., Imaduddin, F. and Jamaluddin, H. (2010) 'Modelling, validation and adaptive PID control with pitch moment rejection of active suspension system for reducing unwanted vehicle motion in longitudinal direction', *International Journal of Vehicle Systems Modelling and Testing*, Vol. 5, No. 4, pp.312–346.

Ali, M.A., Kim, C., Kim, S., Khan, A.M., Iqbal, J., Khalil, M.Z., Lim, D. and Han, C. (2017) 'Lateral acceleration potential field function control for rollover safety of multi-wheel military vehicle with in-wheel-motors', *International Journal of Control*, *Automation and Systems*, Vol. 15, No. 2, pp.837–847.

Aparow, V.R., Hudha, K., Kadir, Z.A., Amer, N.H., Abdullah, S. and Megat Ahmad, M.M.H. (2016) 'Identification of an optimum control algorithm to reject unwanted yaw effect on wheeled armored vehicle due to the recoil force', *Advances in Mechanical Engineering*, Vol. 9, No. 1, pp.1–16.

Ataei, M., Khajepour, A. and Jeon, S. (2019) 'A general rollover index for tripped and un-tripped rollovers on flat and sloped roads', *Proceedings of the Institution of Mechanical Engineers, Part D: Journal of Automobile Engineering*, Vol. 233, No. 2, pp.304–316.

Barethiye, V.M., Pohit, G. and Mitra, A. (2017) 'Analysis of a quarter car suspension system based on nonlinear shock absorber damping models', *International Journal of Automotive and Mechanical Engineering*, Vol. 14, No. 3, pp.4401–4418.

Chen, Q., Zhang, Y., Zhu, C., Wu, J. and Zhuang, Y. (2020) 'A sky-hook sliding mode semiactive control for commercial truck seat suspension', *Journal of Vibration and Control*, Vol. 27, Nos. 11–12, pp.1201–1211.

Chen, Y., Peterson, A.W. and Ahmadian, M. (2019) 'Achieving anti-roll bar effect through air management in commercial vehicle pneumatic suspensions', *Vehicle System Dynamics*, Vol. 57, No. 12, pp.1775–1794.

Chen, Y., Peterson, A.W., Zhang, C. and Ahmadian, M. (2019) 'A simulation-based comparative study on lateral characteristics of trucks with double and triple trailers', *International Journal of Vehicle Safety*, Vol. 11, No. 2, pp.136–157.

Ervin, R.D. (1983) *Influence of Size and Weight Variables on the Stability and Control Properties of Heavy Trucks*, Vol. 1, Final report.

Ervin, R.D. and Guy, Y. (1986) 'Influence of weights and dimensions on the stability and control of heavy trucks in Canada' – Part 1, *Transportation Research Board (TRB) Annual Meeting*, Ottawa, Canada.

Hamed, M. and Elrawemi, M. (2018) *Effects of Spring Stiffness on Suspension Performances Using Full Vehicle Models*, AIJR Publisher, 25–27 September, UK.

Han, I. and Rho, K. (2017) 'Characteristic analysis of vehicle rollover accidents: rollover scenarios and prediction/warning', *International Journal of Automotive Technology*, Vol. 18, No. 3, pp.451–461.

He, Y., Yan, X., Lu, X-Y., Chu, D. and Wu, C. (2019) 'Rollover risk assessment and automated control for heavy duty vehicles based on vehicle-to-infrastructure information', *IET Intelligent Transport Systems*, Vol. 13, No. 6, pp.1001–1010.

Kazemian, A.H., Fooladi, M. and Darijani, H. (2017) 'Rollover index for the diagnosis of tripped and untripped rollovers', *Latin American Journal of Solids and Structures*, Vol. 14, No. 11, pp.1979–1999.

Kemp, R.N., Chinn, B.P. and Brock, G. (1978) 'Articulated vehicle roll stability: methods of assessment and effects of vehicle characteristics', *Transport and Road Research Laboratory: TRRL Laboratory Report*, p.788.

Li, L., Coskun, S., Zhang, F., Langari, R. and Xi, J. (2019) 'Energy management of hybrid electric vehicle using vehicle lateral dynamic in velocity prediction', *IEEE Transactions on Vehicular Technology*, Vol. 68, No. 4, pp.3279–3293.

Ni, Z., Zhu, S. and He, Y. (2020) 'A comparison of test manoeuvres for determining rearward amplification of articulated heavy vehicles', *International Journal of Heavy Vehicle Systems*, Vol. 27, No. 4, pp.405–421.

Nie, S., Zhuang, Y., Liu, W. and Chen, F. (2017) 'A semi-active suspension control algorithm for vehicle comprehensive vertical dynamics performance', *Vehicle System Dynamics*, Vol. 55, No. 8, pp.1099–1122.

Papaioannou, G., Koulocheris, D. and Velenis, E. (2021) 'Skyhook control strategy for vehicle suspensions based on the distribution of the operational conditions', *Proceedings of the Institution of Mechanical Engineers*, *Part D: Journal of Automobile Engineering*, Vol. 235, Nos. 10–11, pp.2776–2790.

Rahimi, S. and Naraghi, M. (2018) 'Design of an integrated control system to enhance vehicle roll and lateral dynamics', *Transactions of the Institute of Measurement and Control*, Vol. 40, No. 5, pp.1435–1446.

Rahmat, M.S., Hudha, K., Kadir, Z.A., Amer, N.H., Nor, N.M. and Choi, S.B. (2021) 'A hybrid skyhook active force control for impact mitigation using magneto-rheological elastomer isolator', *Smart Materials and Structures*, Vol. 30, No. 2, pp.1–17.

Ramakrisna, S., Reddy, B.R.H., Akhil, B. and Kumar, B.P. (2017) 'A review on anti-roll bar used in locomotives and vehicles', *International Journal of Current Engineering and Technology*, Vol. 7, No. 3, pp.838–841.

Ružinskas, A. and Sivilevičius, H. (2017) 'Magic formula tyre model application for a tyre-ice interaction', *Procedia Engineering*, Vol. 187, pp.335–341.

Salaani, M.K. and Elsasser, D.H. (2017) 'Heavy vehicle hardware-in-the-loop crash avoidance safety system simulation with experimental validation', *Proc. 25th Int. Tech. Conf. Enhanced Saf. Vehicles (ESV) Nat. Highway Traffic Saf. Admin*, Michigan, USA, pp.1–8.

Sert, E. and Boyraz, P. (2017) 'Optimization of suspension system and sensitivity analysis for improvement of stability in a midsize heavy vehicle', *Engineering Science and Technology*, *an International Journal*, Vol. 20, No. 3, pp.997–1012.

Wang, Q. and He, Y. (2016) 'A study on single lane-change manoeuvres for determining rearward amplification of multi-trailer articulated heavy vehicles with active trailer steering systems', *Vehicle System Dynamics*, Vol. 54, No. 1, pp.102–123.

Yoon, D-S., Kim, G-W. and Choi, S-B. (2021) 'Response time of magnetorheological dampers to current inputs in a semi-active suspension system: modeling, control and sensitivity analysis', *Mechanical Systems and Signal Processing*, Vol. 146, p.106999.

Yussof, M.A.M., Amer, N.H., Kadir, Z.A., Hudha, K., Adnan, M.N.H. and Aparow, V.R. (2020) 'Modeling and verification of truck handling model due to steering wheel input', *2020 16th IEEE International Colloquium on Signal Processing and Its Applications (CSPA)*, Langkawi, Malaysia, pp.131–135.

Žuraulis, V. and Kilikevičius, A. (2019) 'Quarter car test rig for extended dynamics research in laboratory conditions', *The IAVSD International Symposium on Dynamics of Vehicles on Roads and Tracks*, Gothenburg, Sweden, pp.1425–1434.